HiSST: 2nd International Conference on
High-Speed Vehicle Science & Technology
16–19 May 2022, Bruges, Belgium

High Heat Flux Testing of Yttria-stabilized Zirconia Coatings on Titanium

Philipp Nieke[1], Steve Matthews[2], Nicholas J. Rattenbury[3] and John E. Cater[4]

Abstract

Thermal barrier coatings are attractive thermal protection materials for hypersonic vehicles. We study Yttria-stabilized-Zirconia coatings on pure Titanium and their performance under heat fluxes relevant to hypersonic flight. Coatings were successfully manufactured by air plasma spray, each consisting of a bond coat and a top coat, made from NiCrAlY alloy powder and Yttria-stabilized Zirconia powder, respectively. The predicted peak heat flux of a hypersonic vehicle is simulated with the help of a custom-built Oxy-Acetylene torch apparatus. Coated and uncoated Titanium substrates are subjected to a cold wall heat flux of 900 kW/m^2 for 60 s. Yttria-stabilized-Zirconia coated specimens show no external damage, and for some, performance metrics are about one third higher than for uncoated samples.

Keywords: *Oxy-Acetylene burner testing, air plasma spray, Titanium, Yttria-stabilized Zirconia, thermal barrier coatings*

Nomenclature

Latin
d – Sample thickness
t – Time
I – Insulation index
P – Insulation-to-density performance
T – Back-face temperature
Greek
ρ – Density

1. Introduction

State-of-the-art aerothermodynamic ground-testing of thermal protection materials is typically conducted in plasma wind tunnels [1]. While these facilities yield the results that are closest to actual flight tests, their operation is expensive and access can be limited [2], [3]. Hence, Oxy-Acetylene torch testing has proven an affordable alternative for high-temperature testing of materials and coatings, especially for initial screening [2]–[4].

Thermal barrier coatings (TBCs) based on Yttria-stabilized Zirconia (YSZ) are widely used in the hot sections of gas turbine engines [5]. Typically, TBCs are thermally sprayed on components made of Nickel-based superalloys (e.g. turbine blades) [6]. However, Zirconia coatings were also considered by researchers for the thermal protection of hypersonic vehicles such as the Hexafly-Int glider [7]–[9]. This experimental vehicle with a length of 3 m is intended to sustain a gliding flight at Mach 8 for several minutes [9]. A published reference trajectory shows a peak stagnation point heat flux of approximately 700 kW/m^2 [8]. For this application, Zirconia coatings would need to be deposited on unusual substrate materials such as Copper or Titanium alloys which constitute the structure of the glider. This could pose a challenge as those substrate materials exhibit different corrosion behaviors than the commonly used Nickel-based superalloys and typical bond coat materials are not optimised for them.

In this paper, we investigate YSZ TBCs on Titanium substrates. Firstly, we examine the coating manufacturing via air plasma spray. In the second part, the performance of the coatings under severe heating is studied using a custom-built Oxy-Acetylene testing apparatus.

[1] *University of Auckland, Department of Engineering Science, New Zealand, p.nieke@auckland.ac.nz*
[2] *University of Auckland, Dept. of Chemical and Materials Engineering, s.matthews@auckland.ac.nz*
[3] *University of Auckland, Department of Physics, New Zealand, n.rattenbury@auckland.ac.nz*
[4] *University of Auckland, Department of Engineering Science, New Zealand, j.cater@auckland.ac.nz*

2. Materials and Methods

2.1. Thermal Barrier Coatings

Degreased commercially pure Titanium (CP-Ti) plates with a thickness of 2.1 mm were used as substrate materials. Substrates were grit blasted with alumina powder prior to coating deposition. A commercially available NiCrAlY alloy powder (Oerlikon Metco, Amdry 963) was used for the bond coat and YSZ powder (Oerlikon Metco, Oerlikon Metco, 204B-NS) for the top coat. The NiCrAlY bond coats were air-plasma-sprayed as per the parameters listed in Table 1. Afterwards, YSZ top coats were sprayed on top of the bond coats. For the top coats, several parameter sets (also provided in Table 1) were screened to achieve various coating thicknesses and morphologies. All coatings were applied using a spray gun traverse speed of 833 mm/s. Coated substrates were sectioned to specimens of 25 x 25 mm^2 for high-temperature testing. For reference, three uncoated CP-Ti specimens of the same size were prepared from a thicker substrate (3.2 mm). Cross-sectional micrographs of all as-sprayed coatings were investigated via optical microscopy (Olympus, DSX1000 with DSX10-XLOB objective) to determine the porosities and the thicknesses. For the porosity analysis, more than 10 images per top coat were recorded and converted to a black and white image. Subsequently, the mean area fraction of the pores and the associated standard deviation were evaluated. It was assumed that the pore area fraction is equal to the pore volume fraction. Separate cross-sectional images (see e.g. Fig. 3) were used to assess the mean coating thicknesses, therefore the distance between substrate and top coat was evaluated at 6 locations of each cross-section.

Table 1. Air plasma spray parameters of bond coats and top coats.

Coat	Passes	Carrier gas	Flow rate	H_2 flow rate	Current	Feed rate	Distance
-	-	-	slpm	slpm	A	g/min	mm
Bond	2	Ar	44	6.5	500	60	120
Top A	10 and 20	Ar	40	6.5	600	60	80
Top B	10 and 20	Ar	44	12	480	30	120
Top C	10 and 20	Ar	40	12	500	60	120
Top D	10 and 20	N_2	35	6.5	500	90	120
Top E	10 and 20	N_2	50	10	450	90	120

2.2. Oxy-Acetylene Testing Apparatus

An Oxy-Acetylene testing apparatus was built at the University of Auckland for reproducible and low-cost material screening at extreme heat fluxes. It consists of a welding torch with a tip diameter of 0.9 mm, a positioning mechanism (comprising a moveable carriage on a rail) and two mass flow controllers (Alicat, MC-20SLPM) to set the flow rates of Oxygen and Acetylene. The carriage features a magnetic interface to accommodate either a sensor or a sample holder module. For the initial characterisation of the testing apparatus, a heat flux sensor module was used. It is equipped with a water-cooled Gardon gauge sensor (Hukseflux, GG01-1000) which allows heat flux measurements up to 1000 kW/m^2. The heat flux is calculated from the measured voltage signal and the sensor's sensitivity: 8.7 $\cdot 10^{-9}$ V/(W/m^2) $\pm$ 0.6 $\cdot 10^{-9}$ V/(W/m^2). Fig. 1 shows the apparatus set up for an axial heat flux scan. The sample holder module features a spring-loaded ceramic clamp to secure the samples and a bracket to fixate a thermocouple at the back-face of the sample (see Fig. 4, left). A mineral insulated type K thermocouple (RS Pro) with a diameter of 0.5 mm was used. Temperature data were recorded with a thermocouple data logger (Pico Technology, TC-08). At first, the Oxy-Acetylene burner was characterised by performing axial scans with the heat flux sensor to determine the gas flow rates and the sample position to achieve the required test heat flux. Subsequently, uncoated and coated specimens were exposed to the burner flame to evaluate their high temperature performance. Table 2 shows the selected parameters for the testing which feature a cold wall heat flux of 900 kW/m^2 and a duration of 60 s. Note that this heat flux was measured only at the center of the flame using the GG01-1000 sensor with a sensing area of 14.5 mm^2. This results in the occurrence of most of the heat input at the center of the specimen.

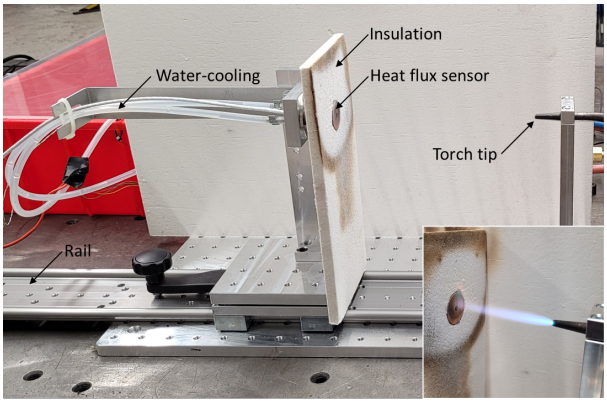

Fig 1. Oxy-Acetylene apparatus with the sensor module mounted. The insert shows a close-up of the heat flux sensor exposed to the flame.

Table 2. Selected condition for high heat flux testing.

Cold Wall Heat flux	Duration	Tip diameter	C_2H_2 flow rate	O_2 flow rate	Distance
kW/m^2	s	mm	slpm	slpm	mm
900	60	0.9	1.0	1.1	130

Performance metrics based on recommendations in ASTM E285-08, are used to compare the results of the coated and uncoated specimens, namely:

- Insulation index $I_{380} = t_{380}/d$,
- Insulation-to-density performance $P_{380} = I_{380}/\rho$,

where t_{380} denotes the time for the temperature increase of the back face by 380 °C, d is the thickness and ρ is the average density of the specimen.

3. Results and Discussion

3.1. Morphology of Deposited Thermal Barrier Coatings

The mean coating thicknesses (bond coat + top coat) including their standard deviations are depicted in Fig. 2. The thickness of the 20-passes variant of each top coat was always approximately twice as large as the 10-passes variant which indicates that the coating thickness scales linearly with the number of passes of the spray gun. Note that the average bond coat thickness of all coatings was 0.072 mm with standard deviation of 0.008 mm. Thicknesses in the range from 0.25 mm to 1.30 mm were produced depending on spray parameters and number of passes. This is larger than the typical thickness range of 0.25 mm to 0.5 mm that is reported for YSZ TBCs in the literature [8]. Fig. 3 contrasts the cross-sections of the thinnest coating (top coat B, 10 passes) and the thickest coating (top coat D, 20 passes).

The porosities of the top coats are presented in Fig. 2 (right) where the error bar denotes the standard deviation. The minimum porosity was 9.31 % for top coat C (20 passes) whereas the largest porosity was 16.75 % for top coat E (20 passes). A decrease in porosity between 10 passes and 20 passes (e.g. for top coat C) could suggest some compaction.

As a result of the various coating thicknesses and small differences in the substrate sizes the specimens mass differs as well which is shown in Fig. 2 (bottom). As all coatings were deposited on thin substrates ($d = 2.1$ mm), only 3 out of 10 coated specimens (top coats A, D and E, 20 passes respectively) had a larger mass than the uncoated reference samples with a thickness of 3.2 mm.

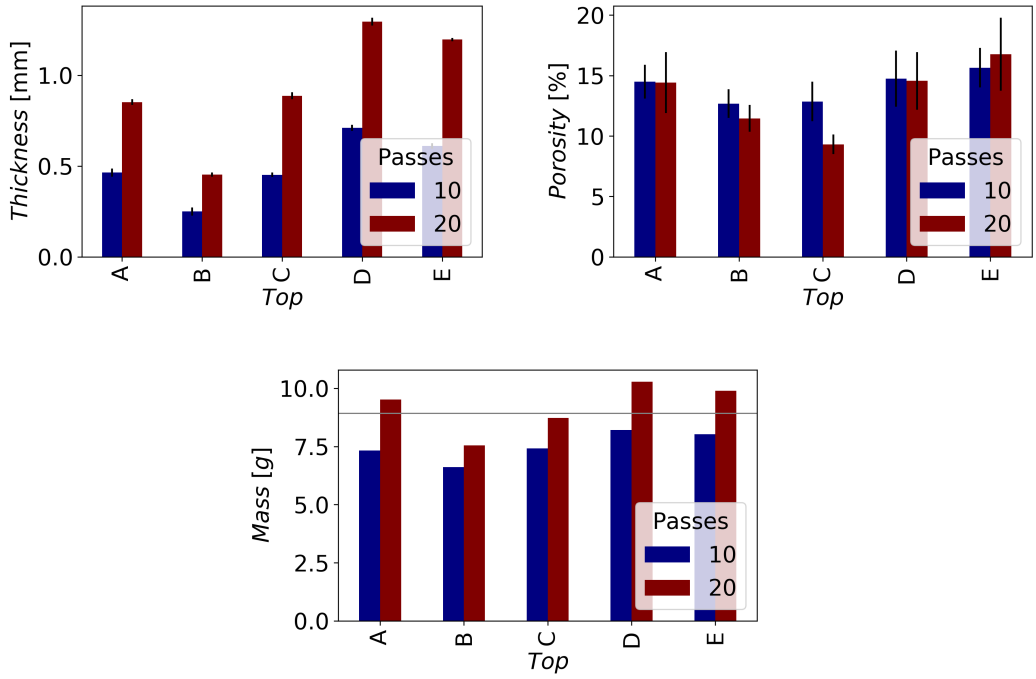

Fig 2. Thickness (left) and porosity (right) of deposited coatings as well as total mass of coated specimens (bottom). The grey line shows the average mass of the uncoated reference samples.

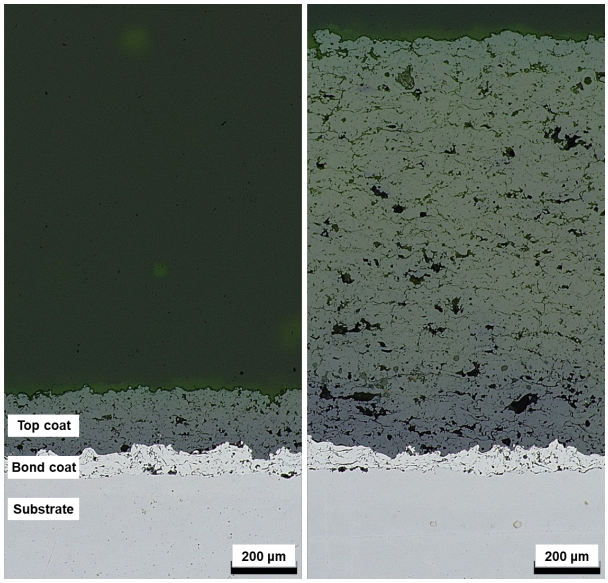

Fig 3. Range of the coating thicknesses: 0.25 mm on the left (top coat B, 10 passes) and 1.30 mm on the right (top coat D, 20 passes). The bond coat thicknesses are approximately equal.

3.2. Oxy-Acetylene Burner Testing

Fig. 4 shows a photo of an uncoated reference sample during the first seconds of a test. It illustrates the local heating by the impinging flame in the center of the sample. It also depicts example back-face temperature plots of an uncoated reference sample, a sample with a thin coating (top coat B, 10 passes)

and a sample with a thick coating (top coat D, 20 passes). The peak temperatures of 880 °C, 1010 °C and 820 °C, respectively, were measured at the end of the tests ($t = 60$ s). Thus, it seems that thermal equilibrium was not fully reached during the testing time. For all times, the temperature of the uncoated reference sample was between the temperatures of the two coated samples. Both the higher mass (higher thermal inertia) as well as a lower thermal conductivity might contribute to the overall lower back-face temperature of the thick coating.

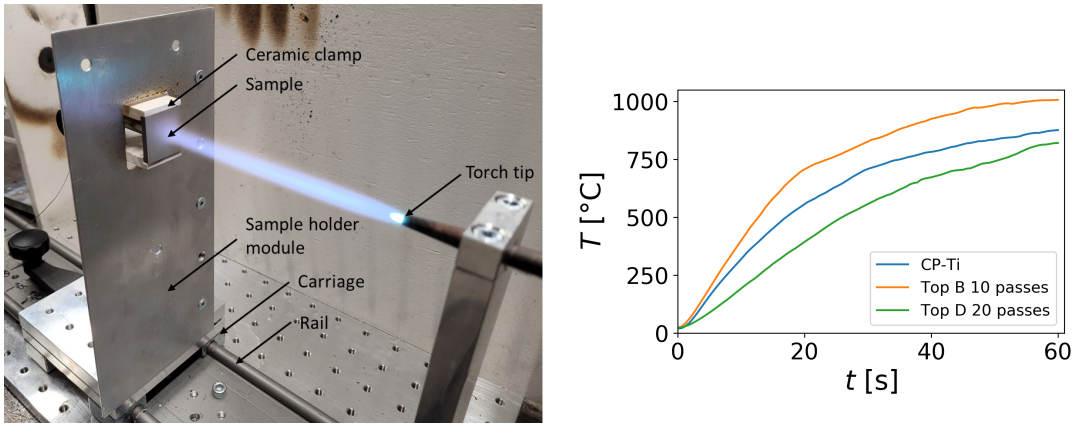

Fig 4. Uncoated reference sample under test (left) and example back-face temperature plots (right).

Therefore, the performance metrics suggested in ASTM E285-08 were used to provide a more nuanced assessment. Fig. 5 shows the insulation index I_{380} and the insulation-to-density performance P_{380} of all coated samples as well as the averages of the uncoated reference samples. In general, all thick coatings (20 passes) performed better than the thin coatings (10 passes) and better than the uncoated reference samples. For example, the thick top coat D exceeds the reference samples by 37 % with respect to the insulation index I_{380} and by 31 % in terms of insulation-to-density performance P_{380}. However, some samples with only a thin coating and relatively low porosity, e.g. top coat B (10 passes) and top coat C (10 passes), performed worse than the uncoated reference samples.

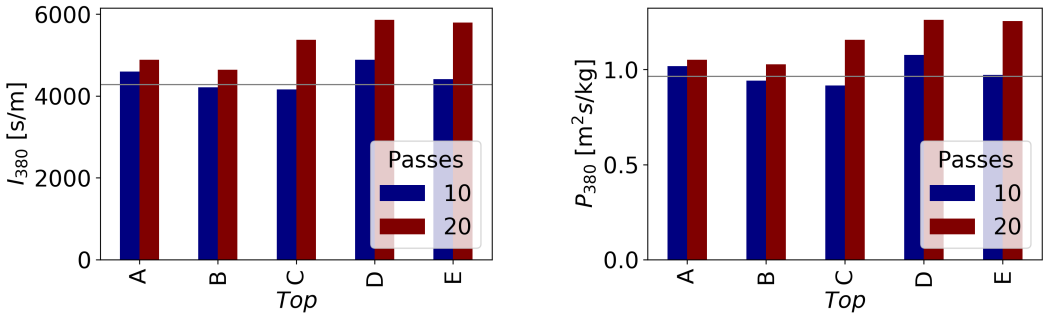

Fig 5. Insulation index (left) and Insulation-to-Density Performance (right) for a back-face temperature increase of 380 °C for all coated samples. The grey line shows the averages of the uncoated reference specimens.

Notably, despite the non-uniform and drastic heating, none of the deposited YSZ coatings failed in terms of cracking or spalling whereas the uncoated reference samples formed an oxide layer that detached upon cooling. The result is visible in the post-test photos of Fig. 6 (left). The uncoated sample showed a circular patch in the center where the oxide scale flaked off. In contrast, the coated sample exhibited no external damage.

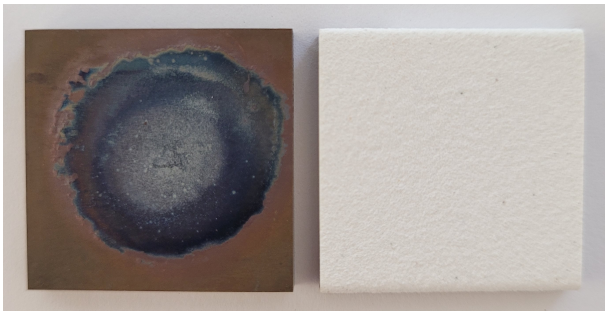

Fig 6. Samples post-test: uncoated CP-Ti (left) and top coat D, 20 passes (right). Note the size of each sample is approximately 25 mm x 25 mm.

3.3. Limitations

The cold wall heat flux produced in these tests is of similar magnitude to the predicted peak heat flux of the reference trajectory of the Hexafly-Int glider. Yet, due to the nature of the tests conducted with combustion gases under ambient conditions, other characteristics of the trajectory could not be replicated, such as the flow velocity and flow chemistry for example. This could influence the formation and stability of oxide scales and would need to be examined further for every specific material used.

Considering the low temperatures in relation to the melting range of YSZ (approximately 2700 °C) and the relatively short timescales, microstructural changes in the YSZ top coat were not expected. However, these conditions could produce reactions between the Titanium substrates and the NiCrAlY bond coats. If long-term stability is important, this behaviour should be the subject of further investigations as well.

4. Conclusion

NiCrAlY bond coats and YSZ top coats were successfully manufactured on pure Titanium substrates using a range of air plasma spray parameters. Coating thicknesses ranging form 0.25 mm to 1.3 mm were produced. Coated and uncoated samples of size 25 mm x 25 mm were tested at ambient conditions using an custom-built Oxy-Acetylene torch apparatus. A cold wall heat flux of 900 kW/m^2 was applied for 60 s resulting in peak back-face temperatures of 820 °C to 1010 °C. Uncoated reference samples formed a flaking oxide scale while coated samples exhibited no external damage. Moreover, samples with a thick coating had an up 37 % higher insulation index and an up to 31 % higher insulation-to-density performance than uncoated reference samples.

5. Acknowledgement

We would like to thank the Technical Services Workshop of the University of Auckland (S. Warrington, P. McKelvie and L. Mclaren) for their contributions to the design, manufacturing and operation of the Oxy-Acetylene testing apparatus. This work was supported by the Endeavour Fund of the Ministry of Business, Innovation & Employment, New Zealand.

References

[1] O. Chazot and F. Panerai, "High-enthalpy facilities and plasma wind tunnels for aerothermodynamics ground testing," in *Hypersonic Nonequilibrium Flows: Fundamentals and Recent Advances*, E. Josyula, Ed. American Institute of Aeronautics and Astronautics, 2014, pp. 471–521.

[2] M. Miller-Oana, P. Neff, M. Valdez, *et al.*, "Oxidation behavior of aerospace materials in high enthalpy flows using an oxyacetylene torch facility," *Journal of the American Ceramic Society*, vol. 98, no. 4, pp. 1300–1307, 2015.

[3] A. Paul, J. Binner, B. Vaidhyanathan, A. Heaton, and P. M. Brown, "Heat flux mapping of oxyacetylene flames and their use to characterise cf-hfb2 composites," *Advances in Applied Ceramics*, vol. 115, no. 3, pp. 158–165, 2016.

[4] W. Tan, M. Adducci, and R. Trice, "Evaluation of rare-earth modified zrb 2–sic ablation resistance using an oxyacetylene torch," *Journal of the American Ceramic Society*, vol. 97, no. 8, pp. 2639–2645, 2014.
[5] C. U. Hardwicke and Y.-C. Lau, "Advances in thermal spray coatings for gas turbines and energy generation: A review," *Journal of Thermal Spray Technology*, vol. 22, no. 5, pp. 564–576, 2013.
[6] R. S. Lima, "Perspectives on thermal gradients in porous zro2-7–8 wt.% y2o3 (ysz) thermal barrier coatings (tbcs) manufactured by air plasma spray (aps)," *Coatings*, vol. 10, no. 9, p. 812, 2020.
[7] R. Scigliano and V. Carandente, "Design analysis of the hexafly-int thermal protection system," in *8th European Workshop on TPS & Hot Structures*, 2016, pp. 19–22.
[8] R. Scigliano, G. Pezzella, M. Marini, S. Di Benedetto, and J. Steelant, "Aerothermal design of the hexafly-int glider," in *AIAA SPACE 2016*, 2016, p. 5627.
[9] J.-Y. Andro, R. Scigliano, A. Kallenbach, and J. Steelant, "Thermal management of the hexafly-int hypersonic glider," in *HiSST*, 2018.